Inorganic Chemistry

Article

pubs.acs.org/IC

An EXAFS Approach to the Study of Polyoxometalate–Protein Interactions: The Case of Decavanadate–Actin

M. Paula M. Marques,[†,‡] Diego Gianolio,[§] Susana Ramos,[∥] Luís A. E. Batista de Carvalho,*[,†] and Manuel Aureliano[†,⊥]

[†]"Química-Física Molecular" R&D Unit, Department of Chemistry, University of Coimbra, 3004-535 Coimbra, Portugal

[‡]Department of Life Sciences, University of Coimbra, 3000-456 Coimbra, Portugal

[§]Diamond Light Source, Harwell Science & Innovation Campus, Didcot OX11 0DE, United Kingdom

[∥]UCIBIO, REQUIMTE, Departamento de Química, Universidade Nova de Lisboa, 2829-516 Caparica, Portugal

[⊥]FCT and CCmar, University of Algarve, 8005-139 Faro, Portugal

Supporting Information

ABSTRACT: EXAFS and XANES experiments were used to assess decavanadate interplay with actin, in both the globular and polymerized forms, under different conditions of pH, temperature, ionic strength, and presence of ATP. This approach allowed us to simultaneously probe, for the first time, all vanadium species present in the system. It was established that decavanadate interacts with G-actin, triggering a protein conformational reorientation that induces oxidation of the cysteine core residues and oxidovanadium (V^{IV}) formation. The local environment of vanadium's absorbing center in the [decavanadate–protein] adducts was determined, a $V–S_{Cys}$ coordination having been verified experimentally. The variations induced in decavanadate's EXAFS profile by the presence of actin were found to be almost totally reversed by the addition of ATP, which constitutes a solid proof of decavanadate interaction with the protein at its ATP binding site. Additionally, a weak decavanadate interplay with F-actin was suggested to take place, through a mechanism different from that inferred for globular actin. These findings have important consequences for the understanding, at a molecular level, of the significant biological activities of decavanadate and similar polyoxometalates, aiming at potential pharmacological applications.

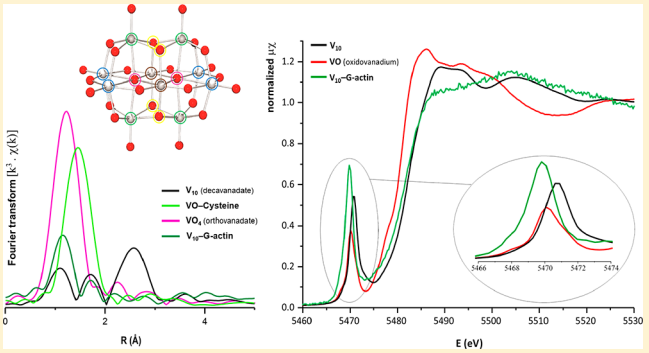

1. INTRODUCTION

Vanadium is a trace element widely distributed in plants and animals. While its essential role for humans is still not fully understood, vanadium compounds are known to be involved in a variety of biological activities and responses (e.g., insulin mimetic, osteogenic, cardioprotective, antitumoral)[1−3] and are therefore the object of intense research, namely regarding potential pharmacological applications. The biochemical role of this type of system is determined by the oxidation state of vanadium, which in turn depends on the intracellular redox potential: V^{IV} (vanadyl or, according to IUPAC, oxidovanadium(IV)), VO^{2+}, henceforth denoted VO (Table 1), occurs under normal metabolic conditions, while V^{V} (orthovanadate, VO_4^{3-}, hereafter denoted VO4) is present in oxidative environments. However, not all biologically relevant properties can be attributed to these oxovanadate forms, as they are also determined by the nature of the ligand(s) coordinated to the vanadium center(s).

Decavanadate, in particular, is a Lindqvist-type isopolyoxometalate (POM) comprising ten distorted-octahedral vanadium(V) centers, in a highly condensed crystal structure[4] ($V_{10}O_{28}^{6-}$, henceforth designated V10). It displays three types of vanadium atoms, previously identified by ^{51}V nuclear magnetic resonance (^{51}V NMR):[5] four equivalent atoms in the border of the equatorial plane (V_A), four equivalent axial V centers above and below the major equatorial plane (V_B), and two equivalent vanadiums in the middle of the equatorial plane (V_C) (Figure 1). Although protonation changes the overall charge and polarity of the decavanadate anion, it does not significantly alter the shapes of the different classes of vanadium atoms within this compact oxoanion.[6]

Decavanadate is known to interact with a wide range of biomolecules, including actin,[7−11] and exerts numerous physiological roles.[7,8,10,12,13] Furthermore, decavanadates are used in catalysis, prevention of corrosion, and smart glasses and are also applied in protein crystallization.[14−17] Regarding the induction of protein crystals, decavanadate (like other POMs[17,18]) fulfills important requisites such as high solubility and stability under most crystallization conditions. In addition,

Received: April 22, 2017
Published: August 31, 2017

DOI: 10.1021/acs.inorgchem.7b01018
Inorg. Chem. 2017, 56, 10893−10903

Table 1. Samples Analyzed in the Present Study

sample composition	physical state	oxidation state of V center	name[a]
metavanadate ($NaVO_3$)	solid	5+	VO3s
decavanadate ($V_{10}O_{28}^{6-}$)	solid	5+	V10s
oxidovanadium (vanadyl, $VOSO_4$)	solid	4+	VOs
decavanadate (0.4 mM), pH 4.0	aqueous solution	5+	V10-4
decavanadate (0.4 mM), pH 4.0, room temp	aqueous solution	5+	V10-4-RT
decavanadate (0.4 mM), pH 7.5	aqueous solution	5+	V10-7
decavanadate (0.4 mM), pH 7.5, room temp	aqueous solution	5+	V10-7-RT
orthovanadate (Na_3VO_4), pH 10.5	aqueous solution	5+	VO4
oxidovanadium+cysteine	aqueous solution	4+	VO-Cys
decavanadate (0.4 mM) + ATP (2 mM)	aqueous solution		V10-ATP
decavanadate (0.4 mM) + G-actin (20 μM)	aqueous solution		V10-G
decavanadate (0.4 mM) + G-actin (20 μM) + KCl (100 mM)	aqueous solution		V10-G-KCl
decavanadate (>0.4 mM) + G-actin (20 μM)	aqueous solution		V10excess-G
decavanadate (0.4 mM) + G-actin (20 μM), room temp	aqueous solution		V10-G-RT
decavanadate (0.4 mM) + G-actin (20 μM) + KCl (100 mM), room temp	aqueous solution		V10-G-KCl-RT
decavanadate (>0.4 mM) + G-actin (20 μM), room temp	aqueous solution		V10excess-G-RT
decavanadate (0.4 mM) + G-actin (20 μM) + ATP (1 mM)	aqueous solution		V10-G-ATP
decavanadate (0.4 mM) + G-actin (20 μM) + ATP (2 mM), room temp	aqueous solution		V10-G-ATP-RT
decavanadate (0.4 mM) + F-actin (20 μM)	aqueous solution		V10-F

[a]All samples are at 37 °C, except when marked RT (room temperature). A 1:10 dilution was carried out for each sample (from 4 mM for V10 and from 40 mM for all other species tested).

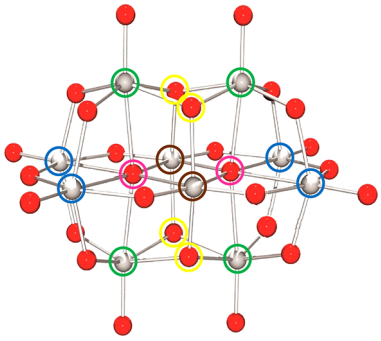

Figure 1. Structural representation of the decavanadate crystal (adapted from ref 5). The gray and red spheres represent vanadium and oxygen atoms, respectively. Three types of vanadium atoms are depicted: four at the left and right (blue, V_A), four at the top and bottom (green, V_B), and two at the center (brown, V_C). Note also a set of four oxygen atoms coordinating unusually with three vanadium centers each (highlighted in yellow), as well as two buried oxygens coordinating six vanadium atoms (highlighted in pink).

decavanadate is known to interact effectively with several proteins, through either electrostatic or hydrogen bond type interactions. However, these specific close contacts have yet to be clarified at the molecular level.[9,10,19]

In addition to the Lindqvist type, other types of POMs display recognized activities against virus and bacteria and more recently toward several types of tumor cells.[20−23] This putative antineoplastic activity is still ill understood, the effect of POMs on the inhibition of tumor proliferation being possibly due to the inhibition of certain enzymes associated with cancer (such as alkaline phosphatases, ecto-nucleotidases, and kinases).[7,21] Regarding the inhibition of virus activity by decavanadate, it has been found to occur either by interaction with proteins in a spatially selective manner[24] or by prevention of the virus−host cell binding.[25] In addition to the success of V10 as an antibacterial and antivirus agent, it presents other health-beneficial roles, the antidiabetic capacity being one of the most widely explored.[13,26] Decavanadate is also a strong enzyme inhibitor (e.g., regarding alkaline phosphatase, adenylate kinase, P-type ATPases, ABC ATPases, F-actin stimulated myosin-ATPase, and ribonuclease activities),[7,8,10,12,27,28] acting through noncovalent interactions that are supposed to be favored by the existence of an ATP binding site within V10 or a V10 back-door binding site.[7,8,12,28−30] This exceptional versatile inhibitory activity is thought to be directly related to a high oxidation ability.[19]

Actin is one of the most abundant proteins in the cellular medium (namely, as part of the cytoskeleton), being associated with crucial biological processes such as muscle contraction, cell adhesion, division, and migration (e.g., in cancer metastasis).[31,32] Globular monomeric actin (G-actin) assembles into F-actin polymers (fibrous species), both forms being in equilibrium within the cell. It was recently found that decavanadate interacts with G-actin at its ATP binding site, inducing an oxidation of the core Cys,[9,33,34] as opposed to the oxidation of two cysteine residues from five upon interaction with F-actin (the exposed Cys-374 and one core Cys).[9,33] This decameric vanadate is the only polyoxovanadate known to promote such an oxidation in actin, with a concomitant V10 reduction from V^V to V^{IV}/vanadyl. This process, however, was found (by electron paramagnetic resonance (EPR) and NMR studies) to be prevented by the presence of ATP, which interferes with the V10−protein interplay.[9,34] In addition, it was observed that actin polymerization (from globular to fibrous actin) is strongly inhibited upon decavanadate interaction with the protein globular form,[35] which can trigger cytoskeleton damage that may be associated with male infertility[36] as well as to prevention of cell migration and invasion (e.g., in glioma and other types of cancer).[37] Furthermore, this interplay leads to decavanadate stabilization, thus suggesting that V10 interacts with specific locations within the protein, protecting this decameric species against conversion to the structurally and functionally distinct lower oxovanadates (vanadium monomer, dimer, or tetramer). The detailed knowledge of the molecular basis of decavanadate−actin interplay[10] and its involvement in the G-actin polymerization process is therefore expected to lead to a better understanding of the cellular processes associated with cell proliferation, adhesion, and migration, namely mechanisms responsible for cancer progression and metastasis,[31,32] thus providing valuable clues for the rational design of improved metal-based anticancer agents. Although the number of studies on vanadium has doubled in the past decade,[7,8,19] reports on vanadium−actin interplay at a

DOI: 10.1021/acs.inorgchem.7b01018
Inorg. Chem. 2017, 56, 10893−10903

molecular level are still scarce and insufficient to explain its significant biological consequences.

The present work reports a simultaneous EXAFS (extended X-ray absorption fine structure) and XANES (X-ray absorption near-edge structure) study aiming at an accurate assessment of decavanadate interaction with G-actin, including a full characterization of the V10−actin binding sites. EXAFS and XANES have proved to be suitable techniques for obtaining detailed local structure information,[38−41] namely on vanadium in protein active centers,[42] and are thus expected to yield reliable information on the exact number and type of neighbor atoms around vanadium, as well as on the metal's oxidation state, in decavanadate−actin adducts (for both the G and F forms), particularly regarding: (i) interaction mode(s), (ii) decavanadate reduction (upon Cys oxidation), (iii) relationship between this interplay and potential conformational changes around the metal (that may explain V10's inhibitory effect toward actin polymerization), and (iv) effect of ATP on the V10−actin coordination. The advantage of the EXAFS and XANES techniques to tackle V10−actin interactions is that they allow probing all vanadium species present in the system simultaneously, while the experimental conditions are varied (regarding pH, ionic strength, temperature, and presence of ATP), in an innovative way. Actually, to the best of our knowledge, this is the first study of decavanadate interaction with actin carried out by EXAFS/XANES.

The data obtained along this study was interpreted in light of the available results already gathered by the authors for this system, by spectroscopic techniques such as ^{51}V NMR, EPR, UV/vis, and Raman.[9,33−36] These results allowed us to achieve an unprecedented characterization, at the molecular level, of the vanadium oxidation state and coordination sphere content in each actin site where interaction takes place. This will pave the way for future studies on V10 interaction with other proteins, where it also exerts significant biochemical effects but no definite knowledge of the binding process is available (e.g., myosin, where it prompts ATPase inhibition).[7,8,12]

2. MATERIALS AND METHODS

2.1. Chemicals. All chemicals used were reagent grade. Ammonium metavanadate was purchased from Riedel de Haen (Germany), while acrylamide, adenosine 5-triphosphate disodium salt (ATP), KCl, $MgCl_2$, and sodium dodecyl sulfate (SDS) were supplied by Sigma-Aldrich Química S.A. (Sintra, Portugal).

2.2. Actin Isolation and Purification. G-actin was extracted from rabbit skeletal muscle following the procedure of Pardee and Spudich.[43] The protein was obtained with a 99% purity (assessed through densitometry analysis upon SDS-polyacrylamide gel electrophoresis).[44] G-actin (42.3 kDa) concentration was determined spectrophotometrically by the method of Gordon and co-workers,[45] using the relationship $\varepsilon_{290}^{1\%} = 0.63$ mg^{-1} ml cm^{-1}. The absorbance value at 290 nm was used, since this is a more reliable measure of protein concentration when ATP levels in the sample and blank are not precisely matched. A 200 μM G-actin stock solution was prepared.

F-actin formation was induced by addition of 100 mM KCl, 1 mM $MgCl_2$, and 1 mM ATP to a G-actin solution, at room temperature.

2.3. Sample Preparation. The solid samples for the EXAFS and XANES experiments were prepared as self-supported pellets using cellulose powder as a blank, the thickness being optimized to obtain an edge jump close to 1.

Vanadate is known to easily oligomerize to decavanadate upon acidification in aqueous solution, and once V10 is formed, it can persist for weeks[5] before decomposing to other vanadate oligomers such as tetra- and divanadate and monomeric vanadate.[7,8,12] Hence, decavanadate solutions were obtained by adjusting the pH of ammonium metavanadate (40 mM) (NH_4VO_3) to 4.0, an orange-yellow color (characteristic of the decameric species) being developed.[7,8,12] Decavanadate stock solutions were kept at 4 °C. For the samples prepared at pH 7.5, 2 mM Tris-HCl was used as a buffer.

A V^{IV}−Cys solution was made by adding decavanadate (4 mM) to solid cysteine (at a 1:1 stoichiometry), which rapidly reduced V10, yielding a blue color indicative of the presence of V^{IV}.

Upon addition of KCl (to a final concentration of 100 mM) to the decavanadate (0.4 mM)/G-actin (20 μM) samples, a certain degree of protein aggregation occurred (after ca. 1.5 h). This can be explained by the interaction of the negatively charged decavanadate anions with cationic amino acid residues within the protein, prompting a neutralization of charges and thus favoring the coalescence of the [V10−G-actin] adducts.

2.4. EXAFS and XANES Experiments. X-ray absorption experiments (simultaneous EXAFS and XANES) were performed at the B18 beamline of the Diamond Light Source.[46] The measurements were carried out using the Cr-coated branch of collimating and focusing mirrors and a Si(111) double-crystal monochromator. The size of the beam at the sample position was ca. 1 mm × 0.5 mm.

Samples were measured both in the solid state and in aqueous solution (in standard liquid cells, containing ca. 0.5 mL), at room temperature and at 37 °C. For the solid samples the data were acquired in transmission mode, with ion chambers before and after the sample filled with appropriate mixtures of inert gases to optimize sensitivity (I_0, 140 mbar of N_2 and 860 mbar of He, resulting in an overall efficiency of 10%; I_t, 100 mbar of Ar and 900 mbar of He, with 80% efficiency). The EXAFS spectra at the V K edge (5465 eV) were obtained from 200 eV before the edge up to 850 eV after the edge (corresponding to 15 Å^{-1} in k space), with a constant step size equivalent to 0.25 eV. EXAFS data on the solutions were collected in fluorescence mode, by means of a 36-element solid-state germanium detector. Data were normalized using the program Athena[47] with a linear pre-edge and polynomial postedge background subtracted from the raw $\ln(I_t/I_0)$ data. Figure S1 in the Supporting Information contains the raw experimental data ($k^3\cdot\chi(k)$), evidencing the high S/N quality of the collected data.

The fit of the experimental EXAFS data was performed by using the program Artemis, which is based on the FEFF code[48] for the theoretical calculation of the scattering path intensities and phases contributing to the EXAFS signal.

In the fitting procedure for V10s, interatomic distances have been calculated for the four different V sites in the system and then grouped if their difference was <0.05 Å. Coordination numbers were calculated by weighted average considering how many times similar bond lengths were found for each crystallographic site and then weighted by the number of V atoms in each site. Debye−Waller factors keep into account the thermal and static disorder of surrounding atoms for each "shell". A higher value of σ^2 corresponds to higher disorder. The same S_0^2 and E_0 values were used for all scattering paths of the photoelectron. Residual differences between experimental data and simulations could be explained by the fact that we did not take into account any multiple scattering path of the photoelectron due to the limited number of parameters that can be used in the fit (number of variables, 20; independent points, 24) as a consequence of the R range (1−3.2 Å) and k range (2−14 Å^{-1}) used.

All XANES fits have been performed in the −8 to +60 eV range excluding the pre-edge peak to avoid influence of geometry in the fit. V10s, VO4, VO3, and VO-Cys were used as standards (not VO, because it is very similar and would cause a high correlation between fit parameters).

3. RESULTS AND DISCUSSION

3.1. Characterization of Vanadate Species. Solid sodium metavanadate ($NaVO_3$, VO3s, V^V), solid decavanadate ($V_{10}O_{28}^{6-}$, V10s, V^V), orthovanadate in aqueous solution (Na_3VO_4, VO4, V^V) and solid vanadium sulfate ($VOSO_4$, oxidovanadium, VOs, V^{IV}) were used as reference samples, while a solution of [oxidovanadium + cysteine] (VO-Cys) was

DOI: 10.1021/acs.inorgchem.7b01018
Inorg. Chem. 2017, 56, 10893−10903

taken as a model of vanadium coordination to cysteine through its sulfur atom (V^{IV}–S_{Cys} coordination) (Table 2 and Figure S2 in the Supporting Information).

Table 2. Results of EXAFS Fits for Standard Samples

standard	CN[a]	dist (Å)	CN	dist (Å)	CN	dist (Å)
VO[b]	1	1.61(2)	4	2.00(2)	1	2.1(1)
VO3[c]	2	1.65(1)	2	1.80(1)		
VO4[d]	1	1.67(4)	3	1.71(1)		

[a]CN denotes coordination number. The fit was performed on the first shell of the EXAFS signal with coordination numbers fixed and all other parameters free. [b]For VO, the total CN is 6 with distances distributed as 1 short, 1 long, and 4 similar. [c]For VO3, the total CN is 4 with distances distributed as 2 short and 2 long. [d]For VO4, the total CN is 4 with distances distributed as 1 short and 3 long.

A good agreement between simulated and experimental data was obtained for solid decavanadate, upon fitting the presently measured EXAFS results on the basis of the reported structure for crystal decavanadate[49] (Table 3 and Figure 2).

Table 3. Selected Bond Distances (in Å) for Decavanadate (Outer and Inner Coordination)

bond	CN[a]	σ^2(Å^2)[b]	R_{eff}[c]	R[d]
V(K)–O_1	1.2	0.005(2)	1.65	1.59(2)
V(K)–O_2	1.6	0.013(5)	1.83	1.77(2)
V(K)–O_3	0.8	0.013(5)	1.92	1.86(2)
V(K)–O_4	1.6	0.013(5)	2.03	1.97(2)
V(K)–O_5	0.8	0.01(1)	2.28	2.3(1)
V(K)–V_1	2.8	0.008(1)	3.10	3.11(2)
V(K)–V_2	1.8	0.015(6)	3.16	3.35(4)

[a]CN denotes coordination number. [b]Debye–Waller factor. [c]Original distances.[49] [d]V–ligand distances refined by the EXAFS fit: χ^2 = 1139; reduced χ^2 = 282; R factor 0.039. The passive electron reduction factor S_0^2 = 0.8 and the edge energy shift E_0 = −9.0 eV were optimized to same value for all listed scattering paths.

Regarding vanadium interactions with cysteine, comparison between the EXAFS profiles for solid oxidovanadium (VOs) and its adduct with cysteine (VO-Cys) reveals slight differences in the first coordination shell: vanadium coordination with cysteine's sulfur atom results in an increase of the first shell intensity at a distance similar to the V–O bond length, without any change in the oxidation state of vanadium (V^{IV}) (Figure 3). This is proposed to be due to an extra coordination of the vanadium center to cysteine's sulfur atom.

3.2. Characterization of Decavanadate Solution Equilibrium. Regarding the vanadate species in aqueous solution under different conditions of pH and temperature, the EXAFS data evidenced that the profiles for V10-4 (0.4 mM V10, pH 4, 37 °C) and V10-7-RT (0.4 mM V10, pH 7.5, room temperature) are similar to that of the solid sample (V10s, oxidation state V), while the results obtained for V10-7 (0.4 mM V10, pH 7.5, 37 °C) are different from those of solid decavanadate (Figure 4) and resemble those of orthovanadate (VO4, V^V). According to the XANES data presently gathered (Table 4), this V10-7 solution contains 81.3% of orthovanadate (V^V) and 18.7% of the reduced species oxidovanadium (V^{IV}), meaning that in the absence of protein all decavanadate species have been decomposed and the solution turns from yellow to colorless. The same should be expected for this solution in the

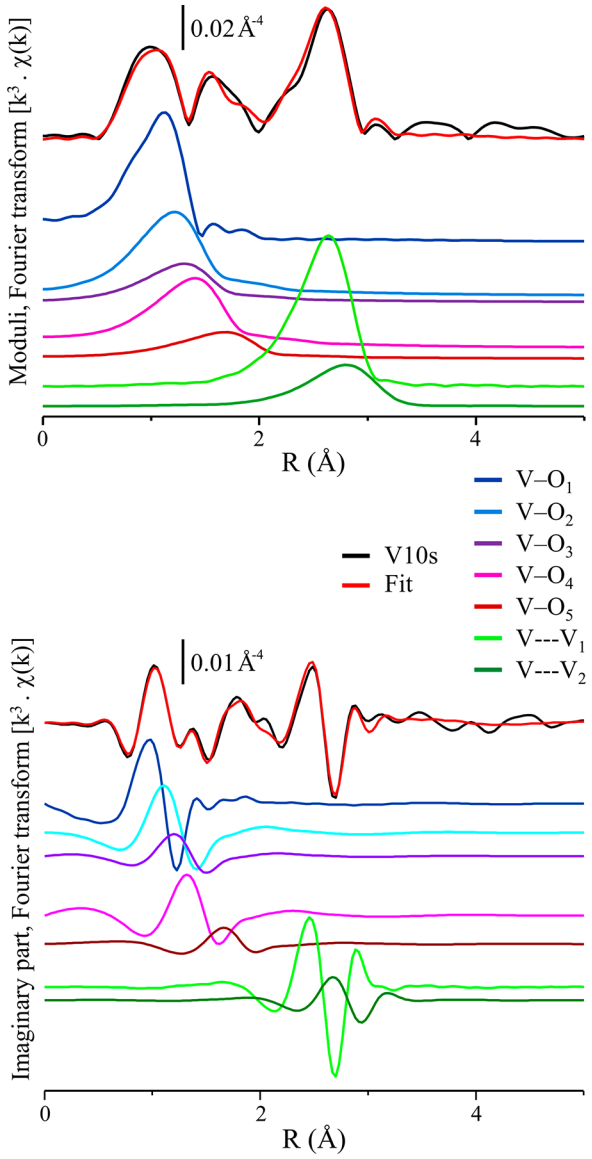

Figure 2. k^3-weighted, phase-uncorrected FT modulus of the V K-edge EXAFS spectra for the solid decavanadate reference: comparison between experimental data (black line) and fit (red line). The contributions from single scattering paths to five different oxygen distances and two different V distances are also shown.

presence of ATP but is not observed. Thus, the combined effect of pH and temperature triggers a change in vanadium's oxidation state (from V^V to V^{IV}) and a subsequent structural reorganization.

Hence, it was shown that decavanadate started to undergo decomposition after about 1 h at pH 7.5 and 37 °C, as opposed to room temperature, for which only V10 was detected for the whole acquisition period (ca. 7 h). Decavanadate solutions had been previously shown (by ^{51}V NMR spectroscopy) to be stable and very homogeneous at room temperature, containing no other vanadate species under these conditions.[7,8,12]

The EXAFS region of the vanadium K-edge spectra of decavanadate (both in the solid state and in aqueous solution) was found to be fitted to two shells: from 0.8 to 1.6 Å, associated with V–O bonds in the first coordination sphere (1.5–2.3 Å), plus a more distant shell from 1.8 to 2.8 Å,

DOI: 10.1021/acs.inorgchem.7b01018
Inorg. Chem. 2017, 56, 10893–10903

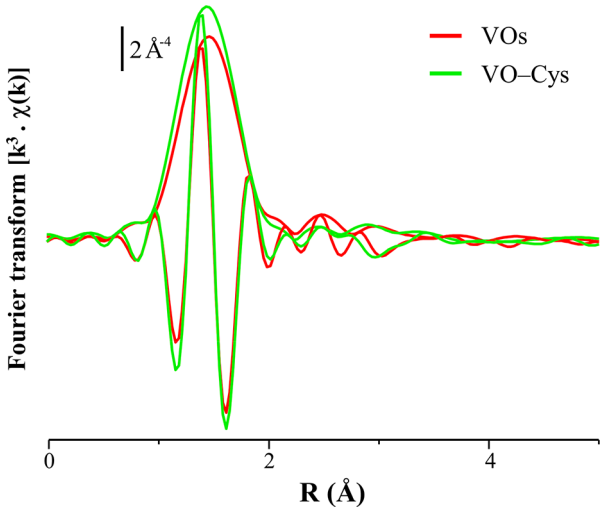

Figure 3. EXAFS Fourier transform $\chi(k)$ data for solid oxidovanadium (VOs) and its adduct with cysteine (VO-Cys).

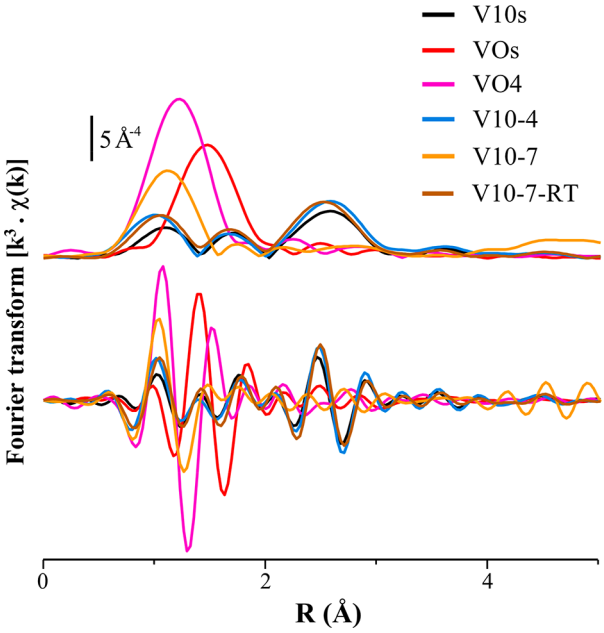

Figure 4. EXAFS Fourier transform $\chi(k)$ data for several vanadate species in solution: decavanadate at pH 4, 37 °C (V10-4), pH 7.5, 37 °C (V10-7), and pH 7.5, room temperature (V10-7-RT); orthovanadate (VO4); oxidovanadium (VO). The profile for solid V10 is also shown (V10s).

corresponding to V···V distances in the outer coordination layer (2.5−3.5 Å) (Table 3).

Table 4 contains the XANES results for V10 solutions at 37 °C and pH 4 (V10-4) or 7.5 (V10-7), with comparison of these with the data obtained for the standard samples decavanadate (V10s, V^V), orthovanadate (VO4, V^V), and metavanadate (VO 3s, V^V). It is clearly shown that pH strongly influences the solution equilibrium, causing the appearance of orthovanadate instead of decavanadate on going from pH 4 to 7.5. However, it does not seem to significantly affect the oxidation state of the vanadium center, since only 18.7% of oxidovanadium (V^{IV}) occurs at pH 7.5, whereas no metavanadate (V^V) is detected.

Regarding the effect of temperature on the solution equilibrium (at physiological pH), it was found that a change from 37 °C to room temperature induces the appearance of V10 (V^V, up to 54.7%), coupled with a marked reduction of orthovanadate, VO4 (V^V, 81.3 to 16.9%), and a small increase in VO-Cys (V^{IV}, 18.7 to 28.4%) (Table 4), mainly reflecting a V10 decomposition to monomeric vanadate (VO4) (for the same vanadium oxidation state).

3.3. Interaction of Decavanadate with Actin. Decavanadate solutions were also analyzed in the presence of actin (20 μM) in either the monomeric G (V10-G) or polymerized F form of actin (V10-F). Regarding the interaction of the V10 polyoxometalate with monomeric G-actin, it is easily inferred that, although the EXAFS profiles of V10s and V10-G-actin at 37 °C were found to be identical up to 1.4 Å (2.0 Å phase corrected), a significant difference was observed around 2.5 Å (2.9 Å phase corrected) (Figure 5A), suggesting that decavanadate's interaction with the globular protein affects mostly the outer sphere of coordination. The V10-G sample contains a mixture of V10 (V^V, 29.3%), orthovanadate (V^V, 53.5%), and oxidovanadium (V^{IV}, 17.1%), as confirmed by the XANES measurements (Table 4). Moreover, no V10 interaction with G-actin was detected at room temperature, the EXAFS profile for V10-G-RT being identical with that from decavanadate (Figure 5B).

In addition, the presence of an excess of decavanadate in the [V10−G-actin] samples in aqueous solution (at 37 °C) was verified to lead to a slight shift of the EXAFS signal in the first coordination sphere to lower coordination distances, probably reflecting a small structural rearrangement around the vanadium center (V10-G vs $V10_{excess}$-G, Figure 5C). An excess of the decavanadate species is also clearly detected (mainly around 2.5 Å, 2.9 Å phase corrected).

It was previously reported that, upon decavanadate interaction with G-actin, oxidation of the G-actin core cysteines takes place simultaneously with vanadyl formation,[9,33,34] but no quantitative data could be obtained. The current study corroborates this type of interplay through the detection, by XANES, of two oxidation states of the vanadium center in V10−G-actin: V^V (deca- and orthovanadate, 82.8%) and V^{IV} (oxidovanadium, 17.1%) (Table 4), only 29.3% of decavanadate (V^V) remaining in solution after interaction with the protein. Actually, the XANES signal detected at ca. 5485 eV is ascribed to the oxidovanadium species (Figure 6), in accordance with reported studies.[50−53] This reduced species is suggested to be formed upon decavanadate binding to one or two Cys residues within globular actin,[9,33,34] as confirmed by comparison of the EXAFS profiles presently obtained for V10-G and VO-Cys, which show similar strong signals in the first coordination shell ascribed to S-bound oxidovanadium (Figure 5A), the slight shift to a lower coordination distance in the [V10−G-actin] adduct evidencing a structural reorganization prompted by decavanadate's interaction with the protein.

Hence, upon V10 interaction with G-actin under physiological conditions, an oxidovanadium(IV) signal was clearly detected by EXAFS and a progressive shift of the edge was observed by XANES on going from decavanadate (V10s) to the V10−protein adduct (V10-G) and oxidovanadium (VOs), which is proof of V10-cysteine binding associated with vanadium reduction. The intensity increase observed in the lower edge peak of the XANES profile is indicative of a loss of symmetry, from V10 to [V10−G-actin] (Figure 6) and possibly to a decrease in vanadium coordination, since this pre-edge intensity was shown to be determined by the size and geometry of the molecular cage surrounding the vanadium absorber.[50]

DOI: 10.1021/acs.inorgchem.7b01018
Inorg. Chem. 2017, 56, 10893−10903

Table 4. XANES Results for the Vanadate Samples in Aqueous Solution Presently Studied[a]

sample	species (%)				*R* factor	red. χ^2
	V10s 5+	VO-Cys 4+	VO4 5+	VO3s 5+		
V10-4 (pH 4, 37 °C)	93.9	0	0	6.1	0.0016	0.00011
V10-7 (pH 7.5, 37 °C)	0	18.7	81.3	0	0.0375	0.00253
V10-7-RT (pH 7.5, room temp)	54.7	28.4	16.9	0	0.0073	0.00035
V10-F (+F-actin, 37 °C)	63.1	22.4	14.5	0	0.0015	0.00009
V10-G (+G-actin, 37 °C)	29.3	17.1	53.5	0	0.0021	0.00013
V10-G-KCl (+G-actin/KCl, 37 °C)	39.1	27.6	33.4	0	0.0079	0.00035
$V10_{excess}$-G (+G-actin/V10, 37 °C)	40.4	24.3	35.3	0	0.0023	0.00013
V10-ATP (+ATP, 37 °C)	70.6	12.1	10.1	7.2	0.0010	0.00007
V10-G-ATP (+G-actin/ATP, 37 °C)	14.0	38.2	47.8	0	0.0061	0.00035
V10-G-RT (+G-actin, room temp)	52.2	22.7	25.2	0	0.0019	0.00015
V10-G-KCl-RT (+G-actin/KCl, room temp)	54.7	31.0	14.3	0	0.0026	0.00019
$V10_{excess}$-G-RT (+G-actin/V10, room temp)	54.6	25.2	20.2	0	0.0032	0.00023
V10-G-ATP-RT (+G-actin/ATP, room temp)	35.1	47.4	17.5	0	0.0028	0.00018

[a] Figure S3 in the Supporting Information.

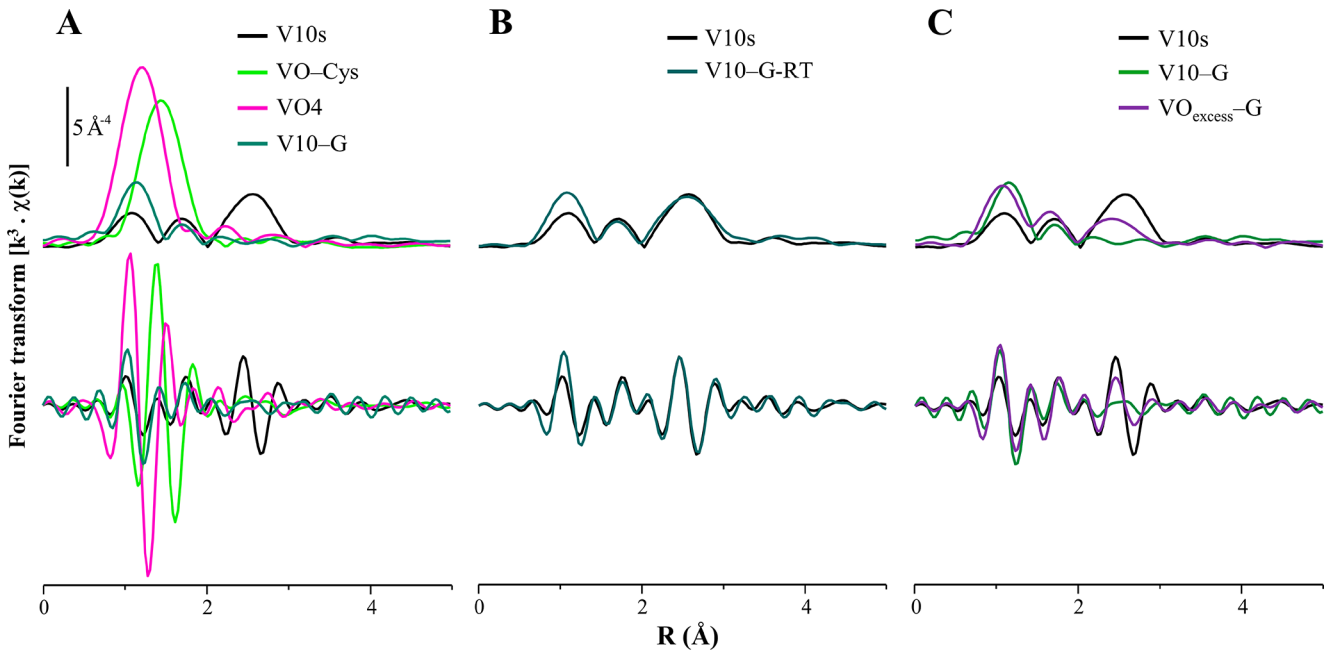

Figure 5. EXAFS Fourier transform $\chi(k)$ data for several vanadate species in solution, in the presence of G-actin: (A) [decavanadate−G-actin] at 37 °C (V10-G), orthovanadate (VO4), [oxidovanadium−cysteine] (VO-Cys), and solid decavanadate (V10s); (B) [decavanadate−G-actin] at room temperature (V10-G-RT) and solid decavanadate (V10s); (C) [decavanadate−G-actin] at pH 7.5, 37 °C (V10-G) and [$decavanadate_{excess}$−G-actin] at 37 °C ($V10_{excess}$-G).

Additionally, the shift to lower frequency detected in the features assigned to V10s and V10-G reflects a distinct structural organization due to decavanadate's coordination to the protein (in its globular form). The maximum frequency of the V10-G peak is identical with that of VO-Cys, unveiling decavanadate coordination to Cys (with a consequent Cys oxidation and V10 reduction).

In sum, the local environment of the vanadium absorbing center within the [V10−G-actin] adduct (in aqueous solution) was determined by EXAFS, and the V−S_{Cys} coordination was verified experimentally at 1.52 Å for V−O in the first coordination sphere (in comparison to 1.78 Å for V−S in the reference sample VO-Cys). This decavanadate interaction with the globular form of actin was found to be very sensitive to temperature: although it is clearly observed at physiological temperature, it does not occur to a significant extent at room temperature. Actually, the EXAFS results obtained for V10-G-RT (V10 + G-actin at room temperature) are identical with those obtained for solid V10 and are distinct from the profile for V10-G (Figure 7).

Regarding decavanadate's interplay with the fibrous form of the protein, it was verified to be quite weak, as reflected in the EXAFS profile obtained for V10-F (V10 + F-actin at 37 °C) in comparison to V10s and V10-G (Figure 7). In fact, the former (V10-F) displays an increase in the first shell second peak, as well as a signal at ca. 1.7 Å (2.0 Å phase corrected) that might reflect some type of interaction between the polyoxovanadate and the polymerized protein. This is corroborated by the XANES data presently gathered (Table 4), 63.1% of V10 having been measured in the presence of F-actin, the other species in solution being oxidovanadium (22.4%) and orthovanadate (14.5%). Interestingly enough, the EXAFS

DOI: 10.1021/acs.inorgchem.7b01018
Inorg. Chem. 2017, 56, 10893−10903

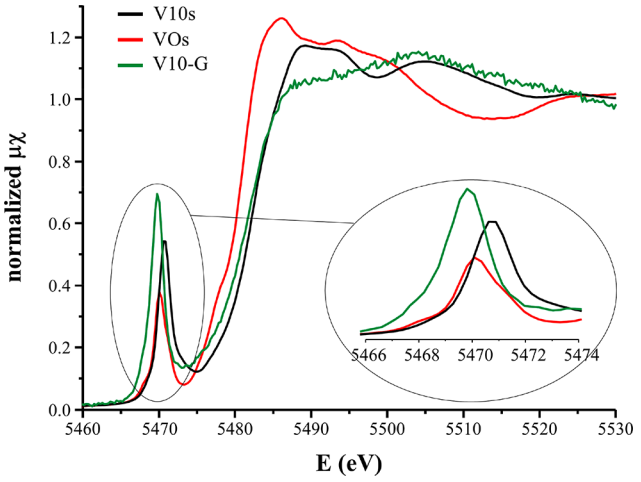

Figure 6. XANES profiles evidencing decavanadate reduction upon interaction with G-actin via Cys residues: [decavanadate−G-actin] solution at 37 °C (V10-G), oxidovanadium (VOs), and solid decavanadate (V10s).

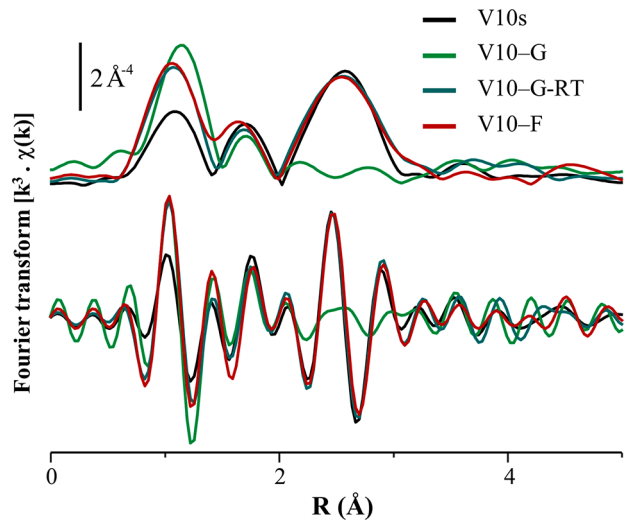

Figure 7. EXAFS Fourier transform $\chi(k)$ data profiles showing decavanadate interplay with actin: [decavanadate−G-actin] at 37 °C (V10-G) and room temperature (V10-G-RT), [decavanadate−F-actin], at 37 °C (V10-F), and solid decavanadate (V10s).

feature at about 1.7 Å (2.0 Å phase corrected) currently detected for V10-F was also present in the V10-G-ATP-RT sample ([V10−G-actin] + ATP at room temperature) (Figure 8), which allows us to suggest that decavanadate is possibly interacting weakly with F-actin through coordination to oxygen center(s) (as in ATP binding), as opposed to cysteine sulfur atoms as in G-actin. These observations are not in total accordance with previous NMR studies,[32] which were unable to expose this specific kind of interaction.

The variations induced in decavanadate's EXAFS profile by the presence of G-actin, at 37 °C, were found to be almost totally reversed by adding ATP to the [V10−protein] adduct, except for the radial distance region between 2 and 3 Å (corresponding to vanadate's outer coordination layer, 2.4−3.4 Å), for which these structural changes were not completely reversed by the presence of the nucleotide (Figure 9A). XANES analysis allowed us to assess that ATP (at physiological temperature) induced a decrease of the V10 phase (to 14%), in

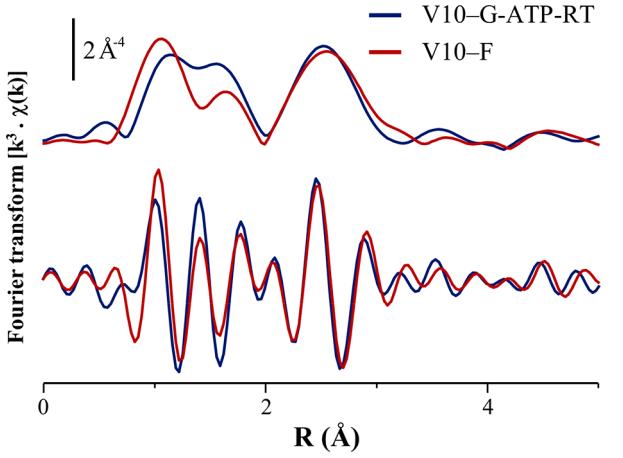

Figure 8. EXAFS Fourier transform $\chi(k)$ data profiles for [decavanadate−G-actin] + AT at room temperature (V10-G-ATP-RT) and [decavanadate−F-actin] at 37 °C (V10-F).

agreement with the appearance of oxidovanadium (V^{IV}, 38.2%) and orthovanadate (V^{V}, 47.8%) (Table 4). In turn, when the results measured at room temperature for [V10 + G-actin] both with and without added ATP were compared, while the general structure of decavanadate was still present, since no interaction between the polyoxametalate and the protein occurs at this temperature, the rise of a second peak in the first shell signal was clearly shown, at a greater distance relative to the V−O bonds in decavanadate (Figure 9B), which may be a direct confirmation of the formation of a new bond. This constitutes solid proof of decavanadate interaction with G-actin at its ATP binding site that appears to be hindered by the preferred coordination of the nucleotide which seems to be favored at physiological temperature. This behavior had been previously suggested by the authors upon studies by NMR, EPR, and fluorescence spectroscopies.[9,33,34]

It may then be concluded that the presence of ATP drastically affects decavanadate−G-actin interactiosn, in different ways depending on the temperature: while at room temperature there is an effect in the first coordination shell, at physiological temperature only the second shell is disturbed, possibly due to the formation of other vanadate species.

Furthermore, comparison between the solutions V10-G-ATP ([V10−G-actin] + ATP, 37 °C) and V10-ATP (V10 + ATP, 37 °C) allowed us to assess a possible coordination between decavanadate and ATP in the absence of the protein, which is proposed to justify the observed increase in the first shell intensity of V10-ATP relative to V10 (Figure 10, around 1 Å), which is possibly due to a higher number of V−O bonds at a bond length of ca. 1.5 Å. However, this should be a weak decavanadate−ATP interaction, in light of the XANES results (Table 4), the major species present in solution still being decavanadate (70.6%). In addition, only in the presence of actin was there a variation in the second coordination shell of the vanadium center, reflecting a distortion of the original decavanadate structure.

3.4. Interaction of Decavanadate with G-actin under Polymerization Conditions. The effect of decavanadate on the G- to F-actin transition process was assessed upon addition of KCl (to a final concentration of 100 mM) to a V10 (0.4 mM)/G-actin (20 μM) solution to yield the V10-G-KCl and V10-G-KCl-RT samples, respectively, at 37 °C and room temperature. Even under these polymerization conditions, there

DOI: 10.1021/acs.inorgchem.7b01018
Inorg. Chem. 2017, 56, 10893−10903

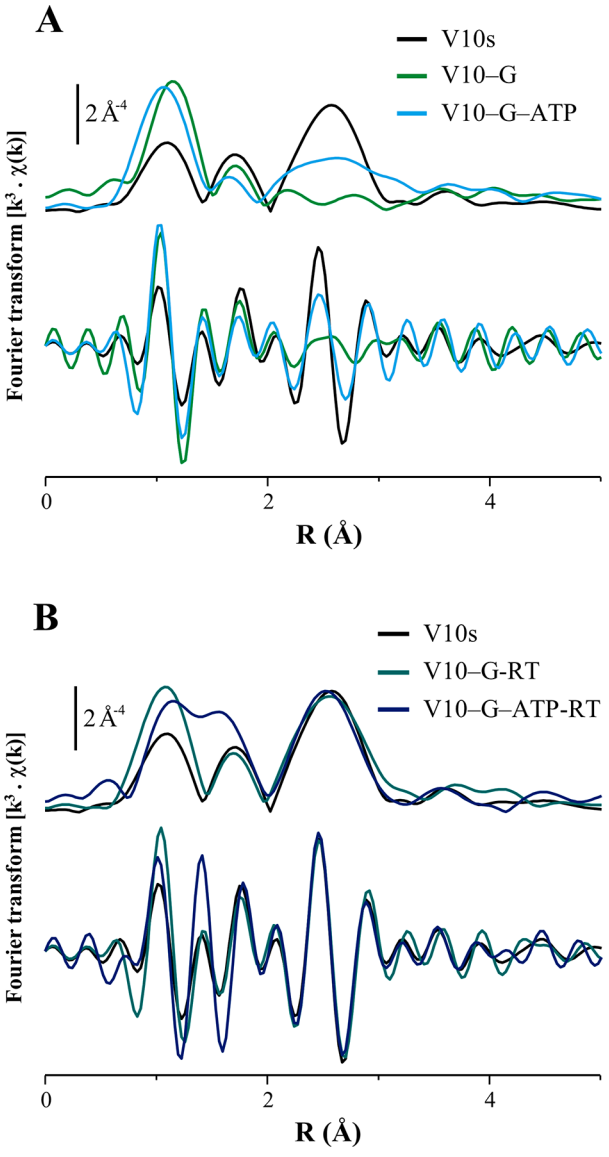

Figure 9. EXAFS Fourier transform $\chi(k)$ data profiles, evidencing the effect of ATP on decavanadate interaction with G-actin for [decavanadate−G-actin] (V10-G), [decavanadate−G-actin] + ATP (V10-G-ATP), and solid decavanadate (V10s): (A) at 37 °C; (B) at room temperature.

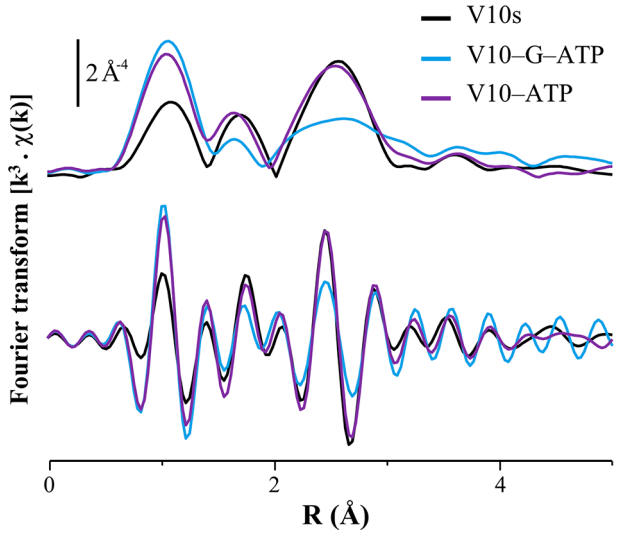

Figure 10. EXAFS Fourier transform $\chi(k)$ data profiles, at 37 °C, showing a possible coordination between ATP and G-actin: [decavanadate−G-actin] + ATP (V10-G-ATP), [decavanadate−ATP] (V10-ATP), and solid decavanadate (V10s).

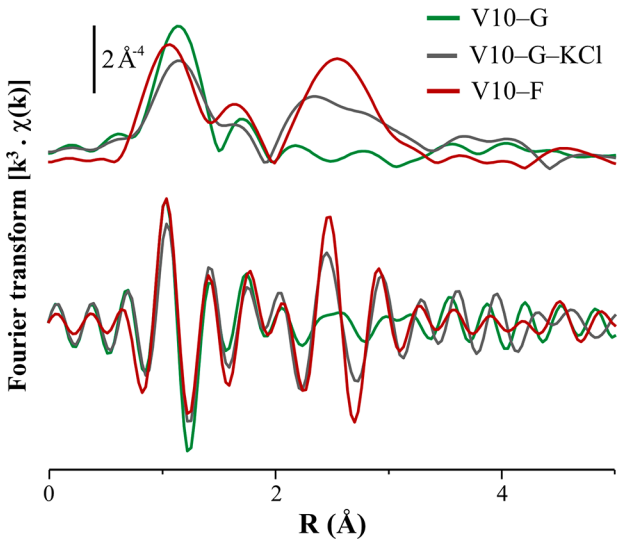

Figure 11. EXAFS Fourier transform $\chi(k)$ data profiles at 37 °C, evidencing the effect of KCl on the G- to F-actin transition: [decavanadate−G-actin] (V10-G), [decavanadate−G-actin] + KCl (V10-G-KCl), and [decavanadate−F-actin] (V10-F).

was no evidence of V10−F-actin formation, as clearly shown in Figure 11.

The presence of the salt, however, was found to have a definite structural effect for the samples at 37 °C, partially disrupting the [V10−G-actin] adduct (Figure 12A). In addition, it was shown to have an effect on vanadium's oxidation state: without KCl more orthovanadate (V^V) was present, while in the presence of KCl less of this species was detected, an increase of about 10% in V10s (V^V) and VO (V^{IV}) being observed (Table 4). At this physiological temperature all of the structures present in solution were found to be different: [V10−G-actin], showing no second shell signal, [$V10_{excess}$−G-actin] (containing an excess of V10), with an EXAFS profile similar to that of decavanadate, and [V10−G-actin] + KCl, displaying an intermediate behavior.

At room temperature, in turn, the effect of the salt seemed to be negligible, so that V10-G-RT and V10-G-KCl-RT yielded an EXAFS profile identical with that of solid decavanadate (Figure 12B).

3.5. Mechanism of Decavanadate Interaction with G-actin. Previous studies[4,7−9,12,28,33,34,54,55] have suggested that the decavanadate anionic species may interact with proteins via hydrogen bonds, by electrostatic means, or even through covalent binding. The current EXAFS and XANES study allowed us to unequivocally observe a V10 interaction with G-actin (via cysteine binding) and detect the subsequent distortion of the original geometry of the polyoxometalate. The synchrotron-based X-ray techniques presently used are able to accurately interrogate a complex system such as the one under study, containing a protein and several vanadium entities in solution, and to enable monitoring all of these species simultaneously while varying the experimental conditions (namely regarding temperature, pH, ionic strength, and

DOI: 10.1021/acs.inorgchem.7b01018
Inorg. Chem. 2017, 56, 10893−10903

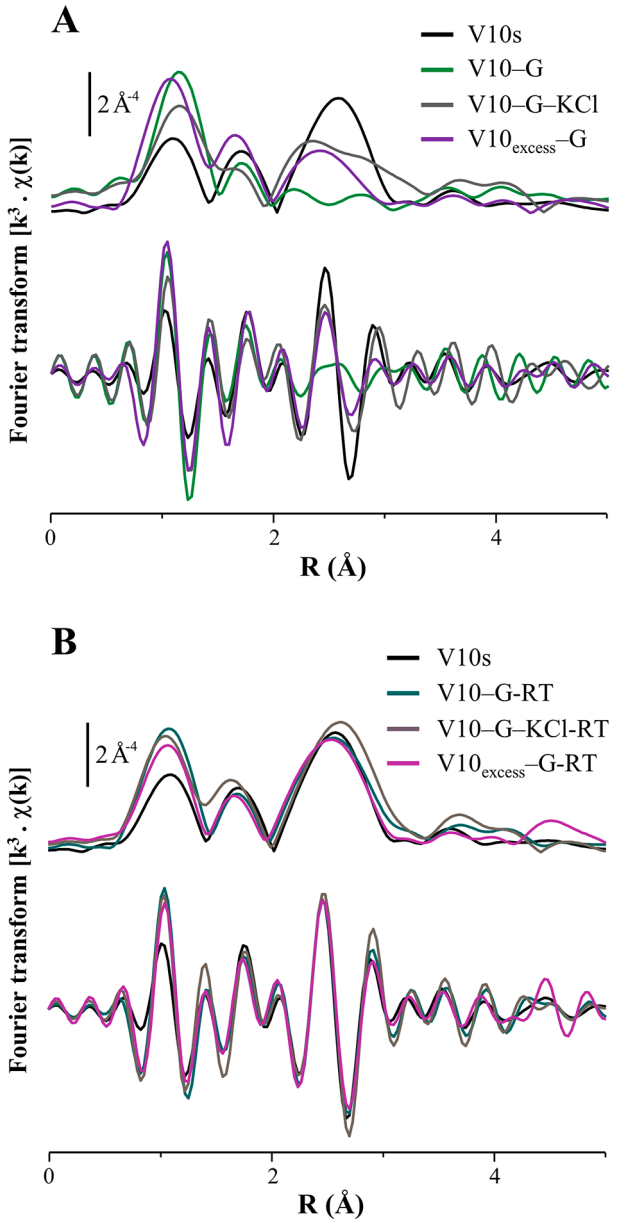

Figure 12. EXAFS Fourier transform $\chi(k)$ data profiles, evidencing the effect of KCl on V10−G-actin interaction, for [decavanadate−G-actin] (V10-G), [decavanadate−G-actin] + KCl (V10-G-KCl), [decavanadate excess−G-actin] ($V10_{excess}$-G), and solid decavanadate (V10s): (A) at 37 °C; (B) at room temperature.

presence of ATP). This is a unique and innovative way of tackling decavanadate−actin interplay at a molecular level, which will greatly contribute to clarify the significant biological roles of this POM.

Upon decavanadate incubation with G-actin a vanadyl signal was observed, identical with that measured for the VO-Cys (V^{IV}-S_{Cys}) reference sample, evidencing decavanadate reduction upon protein interaction, suggested to be due to oxidation of the protein core cysteines as previously described.[33] Indeed, the thiol groups (−SH) of the cysteine residues are the sites most prone to oxidation within the peptide chain, which renders them very suitable biomarkers of redox changes (and consequent conformational rearrangements) experienced by a given protein. In the presence of ATP, G-actin retains all Cys residues in their native redox state, whereas in the presence of V10 one of the cysteines located in the hydrophobic core of the globular protein undergoes oxidation.[9,33] Upon decavanadate interaction with G-actin, the cysteine that is exposed to the solvent, the so-called "fast" cysteine (Cys-374), remains in its reduced form,[9,33] suggesting that the V10 binding site (at the ATP binding location) is too far away to induce its oxidation. Furthermore, the number of cysteine residues exposed to the solvent in globular actin is reported to depend on the presence and nature of the bound nucleotide,[56] whereas it was demonstrated that ATP removal triggers a slow structural transition of the protein that exposes one second thiol group (from Cys-10) to the solvent.[57]

4. CONCLUSIONS

A combined EXAFS and XANES study of the decavanadate−actin interplay, under different conditions (pH, temperature, ionic strength, and presence of ATP), allowed an innovative quantitative assessment of the V10 anion interaction with this protein (in both the globular and polymerized forms), as well as the detection of distinct vanadium species and oxidation states in solution upon protein interaction (decavanadate (V^V), orthovanadate (V^V), and oxidovanadium (V^{IV})).

In light of these data, it was established that decavanadate interacts with globular actin at its ATP binding site, a V−S_{Cys} coordination having been verified for the first time. This triggers a protein conformational reorientation that induces oxidation of the cysteine core residues and subsequent oxidovanadium (V^{IV}) formation (evidencing decavanadate reduction upon protein interaction), these changes being proposed to compromise functional activity. The presently revealed high effect of decavanadate on actin is proposed to be due to the fast equilibrium between this vanadium cluster and the biomolecule. The oxidation state of the vanadium center in the V10−G-actin adduct was identified, both V^V and V^{IV} species having been detected by XANES. The local environment of vanadium's absorbing center in the [V10−protein] adducts was unequivocally assessed, for the different conditions tested, as well as the parameters of the nearest coordination shell around V^V: namely, the number and type of neighbor atoms (oxygen, sulfur, and/or vanadium) and their distance from the selected center. V10−G-actin coordination was shown to be hindered by the presence of ATP in solution (possibly because both species compete for the same binding site). In contrast to G-actin, decavanadate interplay with the fibrous form of the protein (F-actin) seems to occur through a different mechanism, suggested to be via the oxygen atoms at the protein ATP binding site.

The results thus gathered constitute a major step forward aiming at the elucidation of this biologically relevant system, which is still poorly understood at the molecular level. Decavanadate−actin coordination has been up to now mostly probed by spectroscopic techniques such as NMR and EPR, which could not yield the detailed information presently obtained simultaneously for the whole range of chemical components that the system encompasses.

The detailed knowledge of the molecular basis of decavanadate−actin interplay and its involvement in the G-actin polymerization process will hopefully allow a better understanding of the wide range of vanadium's biological activities as well as the mechanism of action underlying decavanadate's antibacterial and antitumor activities. Furthermore, the present experiment paves the way for future studies on polyoxometalate interactions with several other proteins

DOI: 10.1021/acs.inorgchem.7b01018
Inorg. Chem. 2017, 56, 10893−10903

where no precise knowledge of the mechanisms underlying the binding process exists. These findings have important consequences for developing relevant pharmacological applications of V10 and other POMs with strong oxidation capability (and therefore with a higher inhibitory activity).

■ ASSOCIATED CONTENT

Supporting Information

The Supporting Information is available free of charge on the ACS Publications website at DOI: 10.1021/acs.inorgchem.7b01018.

EXAFS and XANES data (PDF)

■ AUTHOR INFORMATION

Corresponding Author

*E-mail for L.A.E.B.d.C.: labc@ci.uc.pt.

ORCID

Luís A. E. Batista de Carvalho: 0000-0002-8059-8537

Notes

The authors declare no competing financial interest.

■ ACKNOWLEDGMENTS

This work was funded by the Portuguese Foundation for Science and Technology-Projects UID/MULTI/00070/2013 and UID/MULTI/04326/2013. Diamond Light Source is acknowledged for time on B18/Core EXAFS (SP12480), under the European Funding programme Calypso FP7.

■ REFERENCES

(1) Crans, D. C.; Smee, J. J.; Gaidamauskas, E.; Yang, L. The Chemistry and Biochemistry of Vanadium and the Biological Activities Exerted by Vanadium Compounds. *Chem. Rev.* **2004**, *104*, 849.

(2) Barrio, D. A.; Etcheverry, S. B. Potential Use of Vanadium Compounds in Therapeutics. *Curr. Med. Chem.* **2010**, *17*, 3632.

(3) Rehder, D. The future of/for vanadium. *Dalton Trans.* **2013**, *42*, 11749.

(4) Debaerdemaeker, T.; Arrietta, J. M.; Amigo, J. M. TetraKis(4-Ethylpyridinium) Dcavanadate. *Acta Crystallogr., Sect. B: Struct. Crystallogr. Cryst. Chem.* **1982**, *38*, 2465.

(5) Aureliano, M.; Ohlin, C. A.; Vieira, M. O.; Marques, M. P. M.; Casey, W. H.; Batista de Carvalho, L. A. E. Characterization of decavanadate and decaniobate solutions by Raman spectroscopy. *Dalton Trans.* **2016**, *45*, 7391.

(6) Sánchez-Lombardo, I.; Baruah, B.; Alvarez, S.; Werst, K. R.; Segaline, N. A.; Levinger, N. E.; Crans, D. C. Size and shape trump charge in interactions of oxovanadates with self-assembled interfaces: application of continuous shape measure analysis to the decavanadate anion. *New J. Chem.* **2016**, *40*, 962.

(7) Aureliano, M.; Crans, D. C. Decavanadate ($V_{10}O_{28}^{6-}$) and oxovanadates: Oxometalates with many biological activities. *J. Inorg. Biochem.* **2009**, *103*, 536.

(8) Aureliano, M.; Ohlin, C. A. Decavanadate *in vitro* and *in vivo* effects: facts and opinions. *J. Inorg. Biochem.* **2014**, *137*, 123.

(9) Ramos, S.; Moura, J. J. G.; Aureliano, M. Actin as a potential target for decavanadate. *J. Inorg. Biochem.* **2010**, *104*, 1234.

(10) Aureliano, M. Recent perspectives into biochemistry of decavanadate. *World J. Biol. Chem.* **2011**, *2*, 215.

(11) Samart, N.; Saeger, J.; Haller, K. J.; Aureliano, M.; Crans, D. C. Interaction of Dacavanadate with Interfaces and Biological Nodel Membrane Systems: Characterization of Soft Oxometalate Systems. *J. Mol. Eng. Mater.* **2014**, *02*, 1440007.

(12) Aureliano, M. Decavanadate: a journey in a search of a role. *Dalton Trans.* **2009**, *42*, 9093.

(13) Treviño, S.; Velázquez-Vázquez, D.; Sánchez-Lara, E.; Diaz-Fonseca, A.; Flores-Hernandez, J. A.; Pérez-Benítez, A.; Brambila-Colombres, E.; González-Vergara, E. Metforminium Decavanadate as a Potential Metallopharmaceutical Drug for the Treatment of Diabetes Mellitus. *Oxid. Med. Cell. Longevity* **2016**, *2016*, 6058705.

(14) Hayashi, Y. Hetero and lacunary polyoxovanadate chemistry: Synthesis, reactivity and structural aspects. *Coord. Chem. Rev.* **2011**, *255*, 2270.

(15) Chen, X.; Yan, S.; Wang, H.; Hu, Z.; Wang, X.; Huo, M. Aerobic oxidation of starch catalyzed by isopolyoxovanadate $Na_4Co(H_2O)_6V_{10}O_{28}$. *Carbohydr. Polym.* **2015**, *117*, 673.

(16) Mohapatra, L.; Parida, K. M. Dramatic activities of vanadate intercalated bismuth doped LDH for solar light photocatalysis. *Phys. Chem. Chem. Phys.* **2014**, *16*, 16985.

(17) Bijelic, A.; Rompel, A. The use of polyoxometalates in protein crystallography − An attempt to widen a well-known bottleneck. *Coord. Chem. Rev.* **2015**, *299*, 22.

(18) Blazevic, A.; Rompel, A. The Anderson-Evans polyoxometalates: From inorganic building blocks via hybrid organic-inorganic structures to tomorrows "Bio-POM. *Coord. Chem. Rev.* **2016**, *307*, 42.

(19) Aureliano, M. Decavanadate Toxicology and Pharmacological Activities: V-10 or V-1, Both or None? *Oxid. Med. Cell. Longevity* **2016**, *2016*, 6103457.

(20) Prudent, R.; Moucadel, V.; Laudet, B.; Barette, C.; Lafanechère, L.; Hasenknopf, B.; Li, J.; Bareyt, S.; Lacote, E.; Thorimbert, S.; Malacria, M.; Gouzerh, P. Cochet, Identification of Polyoxometalates as Nanomolar Noncompetitive Inhibitors of Protein Kinase CK2. C. *Chem. Biol.* **2008**, *15*, 683.

(21) Lee, S. Y.; Fiene, A.; Li, W.; Hanck, T.; Brylev, K. A.; Fedorov, V. E.; Lecka, J.; Haider, A.; Pietzsch, H. J.; Zimmermann, H.; Sévigny, J.; Kortz, U.; Stephan, H.; Müller, C. E. Polyoxometalates—Potent and selective ecto-nucleotidase inhibitors. *Biochem. Pharmacol.* **2015**, *93*, 171.

(22) She, S.; Bian, S.; Huo, R.; Chen, K.; Huang, Z.; Zhang, J.; Hao, J.; Wei, Y. Degradable Organically-Derivatized Polyoxometalate with Enhanced Activity against Glioblastoma Cell Line. *Sci. Rep.* **2016**, *6*, 33529.

(23) Solé-Daura, A.; Goovaerts, V.; Stroobants, K.; Absillis, G.; Jiménez-Lozano, P.; Poblet, J. M.; Hirst, J. D.; Parac-Vogt, T. N.; Carbó, J. J. Probing Polyoxometalate−Protein Interactions Using Molecular Dynamics Simulations. *Chem. - Eur. J.* **2016**, *22*, 15280.

(24) Douglas, T.; Young, M. Host−guest encapsulation of materials by assembled virus protein cages. *Nature* **1998**, *393*, 152.

(25) Rhule, J. T.; Hill, C. L.; Judd, D. A.; Schinazi, R. F. Polyoxometalates in Medicine. *Chem. Rev.* **1998**, *98*, 327.

(26) Pereira, M. J.; Carvalho, E.; Eriksson, J. W.; Crans, D. C.; Aureliano, M. Effects of decavanadate and insulin enhancing vanadium compounds on glucose uptake in isolated rat adipocytes. *J. Inorg. Biochem.* **2009**, *103*, 1687.

(27) Boyd, D. W.; Kustin, K.; Niwa, M. Do vanadate polyanions inhibit phosphotransferase enzymes? *Biochim. Biophys. Acta, Protein Struct. Mol. Enzymol.* **1985**, *827*, 472.

(28) Pezza, R. J.; Villarreal, M. A.; Montich, G. G.; Argarana, C. E. Vanadate inhibits the ATPase activity and DNA binding capability of bacterial MutS. A structural model for the vanadate−MutS interaction at the Walker A motif. *Nucleic Acids Res.* **2002**, *30*, 4700.

(29) Tiago, T.; Martel, P.; Gutiérrez-Merino, C.; Aureliano, M. Binding modes of decavanadate to myosin and inhibition of the actomyosin ATPase activity. *Biochim. Biophys. Acta, Proteins Proteomics* **2007**, *1774*, 474.

(30) Arefian, M.; Mirzaei, M.; Eshtiagh-Hosseini, H.; Frontera, A. A survey of different roles of polyoxometalates in their interaction with amino acids, peptides and proteins. *Dalton Trans.* **2017**, *46*, 6812.

(31) Stevenson, R. P.; Veltman, D.; Machesky, L. M. Actin-bundling proteins in cancer progression at a glance. *J. Cell Sci.* **2012**, *125*, 1073.

(32) Ampe, C.; Machesky, L. M.; Nyitrai, M. Biophysical Approaches for Investigation of the Cytoskeleton. A Special Issue Stemming from Research Presented at the 2012 ECF Meeting: A FEBS/EMBO Workshop Lecture Course in Pécs, Hungary. *Cytoskeleton* **2013**, *70*, 539.

DOI: 10.1021/acs.inorgchem.7b01018
Inorg. Chem. 2017, 56, 10893−10903

(33) Ramos, S.; Duarte, R. O.; Moura, J. J. G.; Aureliano, M. Decavanadate interactions with actin: cysteine oxidation and vanadyl formation. *Dalton Trans* **2009**, 7985.
(34) Ramos, S.; Moura, J. J.G.; Aureliano, M. Recent advances into vanadyl, vanadate and decavanadate interactions with actin. *Metallomics* **2012**, *4*, 16.
(35) Ramos, S.; Manuel, M.; Tiago, T.; Duarte, R. O.; Martins, J.; Gutiérrez-Merino, C.; Moura, J. J. G.; Aureliano, M. Decavanadate interactions with actin: Inhibition of G-actin polymerization and stabilization of decameric vanadate. *J. Inorg. Biochem.* **2006**, *100*, 1734.
(36) Rodríguez-Lara, V.; Morales-Rivero, A.; Rivera-Cambas, A. M.; Fortoul, T. I. Vanadium inhalation induces actin changes in mice testicular cells. *Toxicol. Ind. Health* **2016**, *32*, 367.
(37) Chintala, S. K.; Kyritsis, A. P.; Mohan, P. M.; Mohanam, S.; Sawaya, R.; Gokslan, Z.; Yung, W. K. A.; Steck, P.; Uhm, J. H.; Aggarwal, B. B.; Rao, J. S. Altered Actin Cytoskeleton and Inhibition of Matrix Metalloproteinase Expression by Vanadate and Phenylarsine Oxide, Inhibitors of Phosphotyrosine Phosphatases: Modulation of Migration and Invasion of Human Malignant Glioma Cells. *Mol. Carcinog.* **1999**, *26*, 274.
(38) *XAFS Techniques for Catalysts, Nanomaterials, and Surfaces*; Iwasawa, Y., Asakura, K., Tada, M., Eds.; Springer: Berlin, 2017.
(39) *X-Ray Absorption and X-ray Emission Spectroscopy: Theory and Applications*; van Bokhoven, J. A., Lamberti, C., Eds.; Wiley: Chichester, U.K., 2016.
(40) Bordiga, S.; Groppo, E.; Agostini, G.; van Bokhoven, J. A.; Lamberti, C. Reactivity of Surface Species in Heterogeneous Catalysts Probed by In Situ X-ray Absorption Techniques. *Chem. Rev.* **2013**, *113*, 1736.
(41) Sarangi, R. X-ray Absorption Near-edge Spectroscopy in Bioinorganic Chemistry: Application to M-O-2 Systems. *Coord. Chem. Rev.* **2013**, *257*, 459.
(42) Christmann, U.; Dau, H.; Haumann, M.; Kiss, E.; Liebisch, P.; Rehder, D.; Santoni, G.; Schulzke, C. Substrate binding to vanadate-dependent bromoperoxidase from *Ascophyllum nodosum*: A vanadium K-edge XAS approach. *Dalton Trans.* **2004**, 2534.
(43) Pardee, J. D.; Aspudich, J. A. Purification of muscle actin. *Methods Enzymol.* **1982**, *85*, 164.
(44) Ramos, S.; Almeida, R. M.; Moura, J. J. G.; Aureliano, M. Implications of oxidovanadium(IV) binding to actin. *J. Inorg. Biochem.* **2011**, *105*, 777.
(45) Gordon, D. J.; Yang, Y. Z.; Korn, E. D. Polymerization of *Acanthamoeba* Actin. *J. Biol. Chem.* **1976**, *251*, 7474.
(46) Dent, A. J.; Cibin, G.; Ramos, S.; Smith, A. D.; Scott, S. M.; Varandas, L.; Pearson, M. R.; Krumpa, N. A.; Jones, C. P.; Robbins, P. E. B18: A Core XAS Spectroscopy Beamline for Diamond, in14th International Conference on X-Ray Absorption Fine Structure (XAFS14). *J. Phys.: Conf. Ser.* **2009**, *190*, 012039.
(47) Ravel, B.; Newville, M. J. *ATHENA, ARTEMIS, HEPHAESTUS*: Data Analysis for X-ray Absorption Spectroscopy using. *J. Synchrotron Radiat.* **2005**, *12*, 537.
(48) Rehr, J. J.; Zabinsky, S. I.; Albers, R. C. High-order multiple-scattering calculations of x-ray-absorption fine structure. *Phys. Rev. Lett.* **1992**, *69*, 3397.
(49) Franco, M. P.; Rüdiger, A. L.; Soares, J. F.; Nunes, G. G.; Hughes, D. L. Crystal structures of two decavanadates(V) with pentaaquamanganese(II) pendant groups: $(NMe_4)_2[V_{10}O_{28}\{Mn(H_2O)_5\}_2]\cdot 5H_2O$ and $[NH_3C(CH_2OH)_3]_2[V_{10}O_{28}\{Mn(H_2O)_5\}_2]\cdot 2H_2O$. *Acta Crystallogr.* **2015**, *E71*, 146.
(50) Wong, J.; Lytle, F. W.; Messmer, R. P.; Maylotte, D. H. K-edge absorption spectra of selected vanadium compounds. *Phys. Rev. B: Condens. Matter Mater. Phys.* **1984**, *30*, 5596.
(51) Nabavi, M.; Taulelle, F.; Sanchez, C.; Verdaguer, M. XANES and ^{51}V NMR Study of Vanadium-oxygen compounds. *J. Phys. Chem. Solids* **1990**, *51*, 1375.
(52) Levina, A.; McLeod, A. I.; Pulte, A.; Aitken, J. B.; Lay, P. A. Biotransformations of Antidiabetic Vanadium Prodrugs in Mammalian Cells and Cell Culture Media: A XANES Spectroscopic Study. *Inorg. Chem.* **2015**, *54*, 6707.
(53) Chen, H.-Y.; Friedl, J.; Pan, C.-J.; Haider, A.; Al-Oweini, R.; Cheah, Y. L.; Lin, M.-H.; Kortz, U.; Hwang, B.-J.; Srinivasan, M.; Stimming, U. In situ X-ray absorption near edge structure studies and charge transfer kinetics of $Na_6[V_{10}O_{28}]$ electrodes. *Phys. Chem. Chem. Phys.* **2017**, *19*, 3358.
(54) Hua, S.; Inesi, G.; Toyoshima, C. Distinct Topologies of Mono- and Decavanadate Binding and Photo-oxidative Cleavage in the Sarcoplasmic Reticulum ATPase. *J. Biol. Chem.* **2000**, *275*, 30546.
(55) Fraqueza, G.; Batista de Carvalho, L. A. E.; Marques, M. P. M.; Maia, L.; Ohlin, C. A.; Casey, W. H.; Aureliano, M. Decavanadate, decaniobate, tungstate and molybdate interactions with sarcoplasmic reticulum Ca^{2+}-ATPase: quercetin prevents cysteine oxidation by vanadate but does not reverse ATPase inhibition. *Dalton Trans.* **2012**, *41*, 12749.
(56) Frieden, C.; Patane, K. Differences in G-actin containing bound ATP or ADP: the magnesium-induced conformational change requires ATP. *Biochemistry* **1985**, *24*, 4192.
(57) Drewes, G.; Faulstich, H. A Reversible Conformational Transition in Muscle Actin is Caused by Nucleotide Exchange and Uncovers Cysteine in Position 10. *J. Biol. Chem.* **1991**, *266*, 5508.

DOI: 10.1021/acs.inorgchem.7b01018
Inorg. Chem. 2017, 56, 10893−10903